DOI: 10.1002/cphc.200800786

Fabrication of Monodisperse Toroidal Particles by Polymer Solidification in Microfluidics

Baoguo Wang,[a, b] Ho Cheung Shum,[a] and David A. Weitz*[a, c]

We describe a new strategy to generate toroidal particles through solidification of droplets of polymer solution in a microchannel. Solidification likely proceeds through phase separation of the polymer solution as the solvent diffuses into the continuous phase; this can lead to a higher local polymer concentration. In axisymmetric laminar flow, fluids at the front and the back of the droplet in the axial direction move at the same velocity as the droplet, leading to a stagnation zone and poorer solvent diffusion. As a result, solidification occurs in a spatially non-uniform fashion, resulting in toroidal particles. Our technique enables the continuous production of toroidal particles that are highly monodisperse in both size and shape.

Anisotropic particles[1–5] have important potential as building blocks for self-assembled materials,[6] imaging probes for therapy[7] and fillers for controlling polymer–nanocomposite rheology and tensile strength.[8] Recent investigations also suggest that particle shape can significantly affect the in vivo performance of particles as drug carriers[9,10] and the catalytic efficiency of particle catalysts in oxygen reduction reactions.[11] However, controlling the shape of polymer particles at the micron scale is a challenge, because of the effect of surface tension, which favors spherical particles.

At present, anisotropic polymer particles are fabricated mainly through self-assembly and lithography. Self-assembly is ubiquitous in nature, and has been exploited to produce various structures such as wormlike micelles,[12] cylindrical nanostructures,[13] doughnut-like particles[14] and hierarchically structured particles.[15] However, it is difficult to arbitrarily control the geometry of a three-dimensional structure with self-assembly.[16] Another common strategy for producing anisotropic particles is based on lithography in microfluidics,[16,17] where solidification of fluid streams can be achieved through photopolymerization reactions or through cooling.[18–20] Polymer particles generated with this strategy usually range from 20 to 1000 μm, and are fabricated with the help of confinement effects of the microchannel walls.[18] While lithographic techniques enable arbitrary control of particle shape, the solidification step often requires specific chemistry. Thus, a general approach for producing monodisperse anisotropic polymer particles remains elusive.

Herein, we present a novel strategy to form anisotropic particles by controlled solidification of polymer solution in microfluidic devices. The use of microfluidic techniques enables us to generate monodisperse droplets of polymer solutions; these can then solidify to form polymer particles after solvent removal. By again exploiting the controlled fluid flow possible with microfluidic devices, we can manipulate the fluid flow across the droplets to induce nonuniform solidification, resulting in toroidal polymer particles. This method is completely general and can be applied to different polymers. It also allows us to freely incorporate functional materials into the polymer network to form functional toroidal particles with specific chemical, physical, or mechanical properties.

A glass microcapillary device[21–24] is used to generate simple emulsion droplets of polymer solutions. The device is assembled by inserting the tip of a tapered capillary tube into a collection tube to form a coflow geometry.[25] Alignment of the tapered capillary and the collection tube is achieved by fitting them into a square capillary whose inner diameter matches their outer diameters. (See the Supporting Information for a detailed description of the device fabrication procedure.) The polymer solution is introduced into the tapered capillary as the dispersed phase while the continuous phase flows through the square capillary in the same direction. In all experiments, *N*,*N*-dimethylformamide (DMF) is used as the solvent for the polymer and poly(dimethylsiloxane) [PDMS] oil as the continuous phase. At the tip of the capillary, the polymer solution form drops in the collection tube. Remarkably, these drops eventually solidify to form monodisperse toroidal particles, as shown in Figure 1. Using this approach, monodisperse polymer particles are generated in the size range of 6–120 μm with different polymers including poly(ether sulfone) [PES], polysulfone [PSF], poly(methyl methacrylate) [PMMA] and poly(vinylidene fluoride) [PVDF].

To investigate the formation mechanism of the toroidal particles, we monitor the motion of the polymer solution droplet in the microchannel with high-speed imaging. Initially, a droplet formed at the tip of the capillary exhibits a translational motion along the axial direction. Due to solvent diffusion into the continuous phase, the droplet gradually decreases in size as it flows downstream. After a specific distance, which depends on droplet size and the nature of the polymer, the droplet suddenly shrinks and starts tumbling while continuing to

[a] *Prof. B. Wang, H. C. Shum, Prof. D. A. Weitz*
School of Engineering and Applied Sciences
Harvard University
Cambridge, MA 02138 (USA)
Fax: (+1) 617-495-0426
E-mail: weitz@seas.harvard.edu

[b] *Prof. B. Wang*
Department of Chemical Engineering
Tsinghua University
Beijing, 100084 (PR China)

[c] *Prof. D. A. Weitz*
Department of Physics
Harvard University
Cambridge, MA 02138 (USA)

Supporting information for this article is available on the WWW under http://dx.doi.org/10.1002/cphc.200800786.

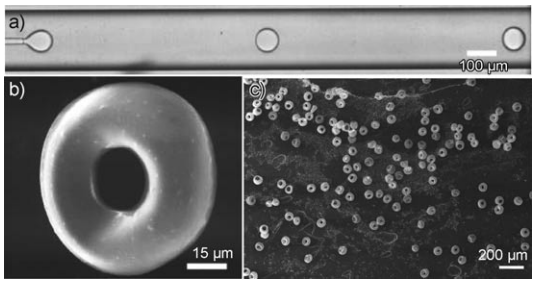

Figure 1. Fabrication of toroidal polymer particles using polymer solidification in an axisymmetric laminar flow field provided by a microcapillary device. a) Droplets of polymer solution being generated inside a microcapillary device. b) Scanning electron microscopy (SEM) image of a typical toroidal polymer particle. The particle was prepared by solidifying a droplet of 10 wt% polysulfone dissolved in DMF, generated with a dispersed phase flow rate, Q_{inner}, of 20 μL hr^{-1} and a continuous phase flow rate, Q_{outer}, of 2500 μL hr^{-1}. c) SEM image of toroidal polysulfone particles prepared under the same conditions as in (b). The particles have an average diameter of 52.9 μm with a standard deviation of 1.5 μm, as shown in Figure S3.

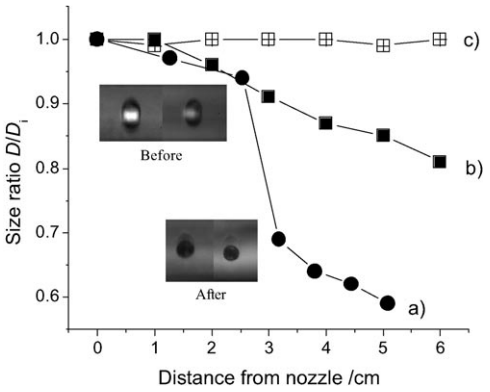

Figure 2. Variation in polymer droplet size with the distance from injection tube exit. Droplet size, D, is expressed as a size ratio relative to the initial droplet size, D_i, at the exit of capillary tube. a) Droplets of polymer solution first decrease slowly in size and then experience a sudden drop at about 2.6 cm from the exit of the capillary tube. The sudden decrease in polymer droplet size indicates solidification of the droplet. The transparent liquid drops, as shown in the inset images labeled "Before", become opaque solid particles following the sudden reduction in size. While the droplets in the inset images labeled "Before" appear non-spherical, they are indeed spherical due to interfacial tension effects. The apparent elongation in the vertical direction is due to the lensing effect associated with imaging through the cylindrical capillary with a wall thickness of 400 μm. The droplets are generated with a dispersed phase flow rate, Q_{inner}, of 50 μL hr^{-1} and a continuous phase flow rate, Q_{outer}, of 5000 μL hr^{-1}. The polymer solution consists of 10 wt% PSF in DMF. b) Droplets of DMF without dissolved polymer decrease in size gradually without the sudden size change as seen in (a). Q_{inner} = 50 μL hr^{-1}, Q_{outer} = 2000 μL hr^{-1}. c) Droplets of polymer solution maintain roughly a constant size when dispersed in PDMS oil saturated by DMF, indicating that the gradual reduction in droplet sizes seen in (a) and (b) results from diffusion of DMF into the surrounding PDMS oil. Q_{inner} = 30 μL hr^{-1}, Q_{outer} = 3000 μL/hr.

translate downstream. We speculate that the interplay between these modes of motion and the rate of droplet solidification determines the final polymer particle structures.

To test this hypothesis, we monitor the size of a droplet of polymer solution along the collection tube. The droplet size is expressed relative to the initial droplet size at the tip of the capillary. A rapid decrease in droplet size is observed about 2.5 cm away from the tip, as shown in the data set labeled (a) in Figure 2. By contrast, no sudden change in droplet size is observed when a DMF droplet without polymer flows down the collection tube (Figure 2b). Nevertheless, the initial slope of this data is similar to that of the data labeled a, up to the abrupt change in droplet size. This indicates that the rate of solvent diffusion into the continuous phase is the same in both cases. We attribute the rapid decrease in droplet size to the solidification of polymer solution. The polymer solution may undergo a phase separation prior to solidification. The phase separation likely leads to the formation of the solidified polymer phase and a DMF-rich phase, which may be removed with the assistance of tumbling motion of the droplet. We also form droplets of polymer solution in PDMS, saturated in advance with DMF, to quench any potential solvent diffusion. In this case, the droplet remains roughly constant in size without solidification, in agreement with our proposition that solidification of the polymer is induced by DMF diffusion into the PDMS. (Figure 2c)

Although DMF is generally considered immiscible with PDMS, a small amount of DMF still diffuses into the bulk PDMS. When a droplet of DMF suspended in PDMS flows in the microchannel, DMF diffuses to the surrounding PDMS until the latter is saturated with DMF. However, due to the difference in the continuous phase velocity along streamlines in different radial positions, DMF in the droplet of polymer solution is removed at a different rate across the droplet surface. In particular, while the rest of the PDMS can move past the DMF droplet, PDMS that is directly in front of and behind the DMF droplet along the axial direction cannot go through the droplet and thus moves at the same velocity as the droplet. This forms local stagnation zones at the front and back of the droplet and the PDMS remains saturated with DMF in these zones; by contrast, PDMS near the circumferential region of the droplet moves away rapidly, keeping the concentration of DMF much lower. Here, the circumferential region refers to the section of the droplet furthest from the mid-line of the cylindrical capillary. Inside the droplet, the polymer concentration becomes higher in the circumferential region since most DMF diffuses away. As a result, solidification of polymer droplet begins at the circumferential surface, after the polymer solution reaches the critical thermodynamic concentration. Polymer in the remaining solution inside the droplet also moves towards the solidified surface, leading to a decrease in polymer concentration in the central region perpendicular to the flow.[27] The originally spherical droplet appears stretched and pinched until the center breaks to form a hole. Eventually all polymer inside the droplet is solidified near the circumferential region, leading to the formation of the doughnut-shaped toroidal structure. The mechanism of toroidal particle formation is completely general and can be applied to different polymers.

Using the system of PES dissolved in DMF, we also demonstrate that both toroidal and spherical particles can be formed with our technique. With a low flow rate of the continuous phase, which leads to a larger droplet of polymer solution, the

droplet solidifies to form a spherical particle, as shown in Figure 3a. We attribute the formation of the spherical particles to the increase in droplet size and concomitant decrease in the

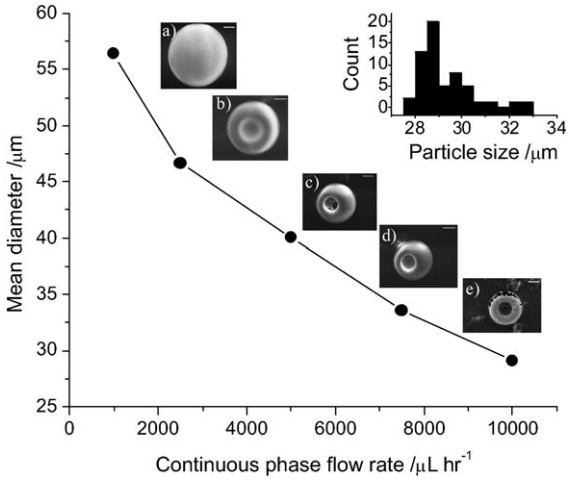

Figure 3. Controllable PES particle size formed by adjusting the continuous phase flow rate at a constant inner flow rate of 30 μL hr^{-1}. The particle diameter decreases with outer phase flow rate. The morphology of the particles also changes with the outer phase flow rate, as shown by the corresponding electron micrographs (a)–(e) next to each data point. Inset: Particle size distribution with Q_{outer} = 10000 μL hr^{-1}. All polymer solutions used consist of 10 wt% PES in DMF. Scale bars on all electron micrographs are 10 μm.

continuous phase flow rates, which results in a slower rate of solvent removal. Since the solidification of the droplets is not completed within the translational motion stage, the ensuing tumbling motion removes any nonuniformity in DMF concentration across the droplet surface, resulting in spherical particles, as shown in Figure 3a. By gradually increasing the flow rate of the continuous phase, we can form particles that range from having two dimples (Figure 3b), to doughnut-shaped to perfect toroidal particles. Alternatively, spherical droplets can also be formed by reducing the polymer concentration, since it then takes a longer time to remove enough solvent to reach the critical concentration for solidification and the tumbling motion prevents the formation of any non-spherical geometries. This behavior has been exploited to fabricate spherical PVDF particles (Figure S6, Supporting Information). The detailed structure of these spherical particles depend on the conditions, such as polymer concentration, under which the particles are formed. By varying the fluid flow rates and polymer concentration, we have also fabricated PMMA particles with different morphologies, as shown in Figure 4. The two scenarios for forming spherical particles are in agreement with our hypothesis that the toroidal structure forms because of a spatially nonuniform solidification step induced by nonuniform solvent diffusion across the polymer solution droplets. Based on these observations, it should also be possible to tune the particle asymmetry by adjusting the critical concentration for solidification through the choice of the chemical nature or molecular weight of the polymer used.

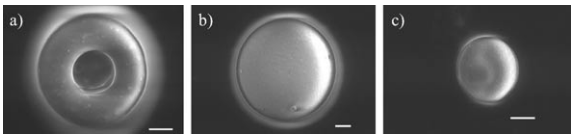

Figure 4. SEM images of various PMMA particle structures obtained under different preparation conditions. a) Particle formed from a droplet of 10 wt% PMMA in DMF with a dispersed phase flow rate, Q_{inner}, of 30 μL hr^{-1} and a continuous phase flow rate, Q_{outer}, of 5000 μL hr^{-1}. b) Particle formed from a droplet of 10 wt% PMMA in DMF. Q_{inner} = 30 μL hr^{-1}, Q_{outer} = 1000 μL hr^{-1}. c) Particle formed from a droplet of 5 wt% PMMA in DMF. Q_{inner} = 30 μL hr^{-1}, Q_{outer} = 5000 μL hr^{-1}. All scale bars are 10 μm.

With our technique, monodisperse toroidal particles of different sizes and different polymers can be formed. The size of the toroidal particles can be tuned by adjusting the flow rate of the continuous phase. The particle size decreases roughly linearly with the flow rate of the continuous phase for a given inner fluid flow rate, as shown in Figure 3. The smallest toroidal particles formed by satellite droplets are about 7 μm in diameter, and the particle sizes that can be readily made with this technique range from several to hundreds of micrometers. In addition, particles generated with this technique are highly monodisperse, as shown in the particle size distribution in Figure 3. The size distribution of the particles formed is determined by the size uniformity of the droplets of polymer solution. Highly monodisperse droplets are produced under the dripping regime while droplets formed in the jetting regime tend to be more polydisperse.[23] Apart from PES, the technique can also be applied to PMMA and PSF to make toroidal particles. The phase separation of these polymers from solution has been widely studied for membrane formation and can be categorized into different phase transitions.[28] Herein, we introduce a novel approach for inducing controlled solidification using microfluidic flow. The broad applicability of the technique is made possible by the use of glass-based devices, which are chemically resistant to most organic solvents used for dissolving polymers.[25] Currently, a single device is capable of producing 10^4–10^5 particles per hour. Productivity can be increased further by parallelization. With appropriate surface modifications for improved chemical resistance,[26] it should also be feasible to use stamped lithography-based microfluidic devices, which can be more easily scaled up to produce many devices in parallel.

The technique can also be used for fabricating composite particles to meet the needs of different applications. We produce composite toroidal particles by adding functional components to the polymer solutions before the microfluidic emulsification step. By dissolving a small amount ($<$ 0.1 wt%) of fluorescein sodium salt or rhodamine B salt in DMF containing PSF or PMMA respectively, fluorescent PSF and PMMA toroidal particles are generated, as shown in Figure 5a,b. The uniform fluorescence across the particles suggests that the fluorescent salt is well dispersed in the polymer matrix of the toroidal particles. Similarly, by suspending hydrophilic magnetic nanoparticles in the polymer solution, magnetic toroidal particles are fabricated, as shown in Figure 5c. Despite the low volume fraction of

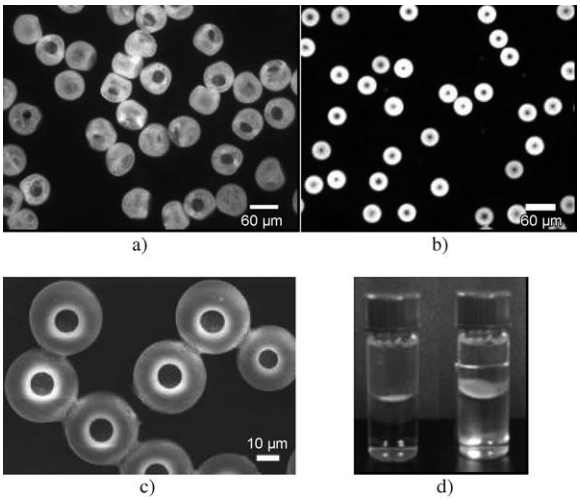

Figure 5. Composite particles with a toroidal structure. a) An optical microscope image of PSF toroidal particles containing fluoresein sodium salt of less than 0.1 wt%. The PSF particles were prepared from a solution of 10 wt% PSF dissolved in DMF. b) An optical microscope image of PMMA toroidal particles containing rhodamine B of less than 0.1 wt%. c) An electron microscope image of PMMA toroidal particles containing 10 nm magnetic particles at approximately 0.5 wt%. The PMMA particles were prepared from a solution of 10 wt% PMMA dissolved in DMF. d) Magnetic toroidal particles are attracted towards a magnet placed behind the glass vial (right), and stay at the interface of the PDMS oil and water in the absence of a magnetic field (left).

magnetic nanoparticles, the resultant particles show a magnetic response and are attracted to a nearby magnet, as seen in Figure 5d. The successful incorporation of different functional components into the polymer toroidal particles highlights the versatility and robustness of this microfluidic approach.

In summary, we introduced a general one-step technique for the continuous fabrication of monodisperse toroidal polymer particles by combining solidification of polymer solutions with microfluidic emulsification. By utilizing the laminar axisymmetric flow in a microchannel, solvent diffusion can be controlled to result in non-uniform solidification of the polymer solution droplets. The technique enables precise tuning of the final particle size and shape, and is applicable for different polymers. We have also shown that composite toroidal particles can be formed by adding additional components into the polymer solution. Our simple and versatile technique provides a novel approach to form these composite particles for specific applications that require complicated toroidal particles. For instance, fluorescent toroidal particles may be used as anisotropic imaging probes for biomedical applications, while magnetic toroidal particles may be embedded in cells for magnetic actuation. Our results demonstrate the concept of shape control by tuning the fluid flow, which may be manipulated appropriately to generate particles with other shapes.

Experimental Section

The continuous phase used in all experiments was PDMS oil (Sigma–Aldrich) with a viscosity of 1 cSt, containing 2 wt% Dow Corning 749 fluid (Dow Corning) as a surfactant; and the solvent used to dissolve all polymers in the experiments was DMF (Sigma–Aldrich) with purity above 99.8 wt%. Four kinds of polymers, PSF (Aldrich, Number average molecular weight, Mn, 16000), PMMA (Aldrich, Mn 120000), PVDF (Aldrich, Mn 107000) and PES (Solvay advanced polymers, Radel A-304P, Mn 18600), were dissolved in DMF to make up the polymer solutions, which were used as the dispersed phase of the emulsions. The concentrations used in the experiments are 0.001 to 12 wt% for PSF, 5 to 10 wt% for PMMA, 4 to 8 wt% for PVDF and 10 wt% for PES. The chemical structures of the PSF and PES used in the experiments are shown in Figure S1 in the Supporting Information. Fluorescein sodium salt (Sigma–Aldrich) was added to a PSF solution and rodamine B (Sigma–Aldrich) was added to a PMMA solution to prepare fluorescent particles. Ferrofluid (EMG 708, Ferrotec) was added to the PMMA solution to prepare magnetic particles.

The injection tube of the microcapillary device was fabricated from a cylindrical capillary with an outer diameter of 1 mm; the tapered shape was prepared by pulling the capillary at 460 °C using a micropipet puller (Sutter Instrument, Model P-97). The collection tube has an inner diameter of 200 μm and an outer diameter of 1 mm. Both the injection tube and the collection tube were inserted into a square capillary with an inner dimension of 1.05 mm (Atlantic International Technologies) for alignment. A transparent epoxy resin was used to seal the tubes where required. Polymer solution was introduced into the device through the tapered end of the injection tube; droplets of the polymer solution formed at the tip of the capillary orifice. The continuous phase was introduced through the gap between the outer square tube and the inner injection tube, and then flowed into the collection tube in a co-flow manner. A schematic of the microcapillary device is shown in Figure S2 in the Supporting Information. Solutions were supplied to the microcapillary device through polyethylene tubing (Scientific Commodities) connected to syringes (Hamilton Gastight). Both fluids were driven by syringe pumps (Harvard Apparatus, PHD 2000 series) with positive displacement. The drop formation was imaged with a high-speed camera (Vision Research) attached to a microscope.

Acknowledgements

This work was supported by BASF, the NSF (DMR-0602684), the Harvard MRSEC (DMR-0820484), the NSFC (20676068) and the Major State Basic Research Development Program of China (973 Program, No. 2003CB615701). B. G. Wang thanks the China Scholarship Council (20076020). PES was generously provided by Solvay Advanced Polymers, L.L.C.

Keywords: colloids · composites · emulsions · particles · polymers

[1] J. W. Kim, R. J. Larsen, D. A. Weitz, *Adv. Mater.* **2007**, *19*, 2005.
[2] O. D. Velev, A. M. Lenhoff, E. W. Kaler, *Science* **2000**, *287*, 2240.
[3] V. N. Manoharan, M. T. Elsesser, D. J. Pine, *Science* **2003**, *301*, 483.
[4] Z. H. Nie, W. Li, M. Seo, S. Q. Xu, E. Kumacheva, *J. Am. Chem. Soc.* **2006**, *128*, 9408.
[5] W. Wei, H. F. Xu, X. Z. Qu, X. L. Ji, W. Jiang, Z. Z. Yang, *Macromol. Rapid Commun.* **2007**, *28*, 1122.
[6] P. F. Noble, O. J. Cayre, R. G. Alargova, O. D. Velev, V. N. Paunnov, *J. Am. Chem. Soc.* **2004**, *126*, 8092.
[7] M. Yoshida, K. H. Roh, J. Lahann, *Biomaterials* **2007**, *28*, 2446.
[8] S. T. Knauert, J. F. Douglas, F. W. Starr, *J. Polym. Sci. Part B: Polym. Phys.* **2007**, *45*, 1882.

[9] J. A. Champion, Y. K. Katare, S. Mitragotri, *J. Controlled Release* **2007**, *121*, 3.
[10] J. A. Champion, S. Mitragotri, *Proc. Natl. Acad. Sci. USA* **2006**, *103*, 4930.
[11] C. Wang, H. Daimon, T. Onodera, T. Koda, A. H. Sun, *Angew. Chem.* **2008**, *120*, 3644; *Angew. Chem. Int. Ed.* **2008**, *47*, 3588.
[12] B. M. Discher, Y. Y. Won, D. S. Ege, J. C.-M. Lee, F. S. Bates, D. E. Discher, D. A. Hammer, *Science* **1999**, *284*, 1143.
[13] X. S. Wang, G. Guerin, H. Wang, Y. S. Wang, L. Manners, M. A. Winnik, *Science* **2007**, *317*, 644; H. G. Cui, Z. Y. Chen, S. Zhong, K. L. Wooley, D. J. Pochan, *Science* **2007**, *317*, 647.
[14] H. A. Wege, A. K. F. Dyab, O. D. Velev, V. N. Paunov, *Phys. Chem. Chem. Phys.* **2007**, *9*, 6300; L. Alexander, K. Dhaliwal, J. Simpson, M. Bradley, *Chem. Commun.* **2008**, 3507; L. A. Connal, G. G. Qiao, *Soft Matter* **2007**, *3*, 837.
[15] J. T. Zhu, R. C. Hayward, *Angew. Chem.* **2008**, *120*, 2143; *Angew. Chem. Int. Ed.* **2008**, *47*, 2113.
[16] R. S. Kane, *Angew. Chem.* **2008**, *120*, 1388; *Angew. Chem. Int. Ed.* **2008**, *47*, 1368.
[17] M. Seo, Z. H. Nie, S. Q. Xu, M. Mok, P. C. Lewis, R. Graham, E. Kumacheva, *Langmuir* **2005**, *21*, 11614.
[18] S. Q. Xu, Z. H. Nie, M. Seo, P. Lewis, E. Kumacheva, H. A. Stone, P. Garstecki, D. B. Weibel, I. Gitlin, G. M. Whitesides, *Angew. Chem.* **2005**, *117*, 734; *Angew. Chem. Int. Ed.* **2005**, *44*, 724.
[19] P. C. Lewis, R. R. Graham, Z. H. Nie, S. Q. Xu, M. Seo, E. Kumacheva, *Macromolecules* **2005**, *38*, 4536.
[20] C. Serra, N. Berton, M. Bouquuey, L. Prat, G. Hadziioannou, *Langmuir* **2007**, *23*, 7745.
[21] A. S. Utada, E. Lorenceau, D. R. Link, P. D. Kaplan, H. A. Stone, D. A. Weitz, *Science* **2005**, *308*, 537.
[22] L. Y. Chu, A. S. Utada, R. K. Shah, J. W. Kim, D. A. Weitz, *Angew. Chem.* **2007**, *119*, 9128; *Angew. Chem. Int. Ed.* **2007**, *46*, 8970.
[23] A. S. Utada, A. F. Nieves, H. A. Stone, D. A. Weitz, *Phys. Rev. Lett.* **2007**, *99*, 094502.
[24] L. Y. Chu, J. W. Kim, R. K. Shah, D. A. Weitz, *Adv. Funct. Mater.* **2007**, *17*, 3499.
[25] A. S. Utada, L. Y. Chu, A. F. Nieves, D. R. Link, C. Holtze, D. A. Weitz, *MRS Bull.* **2007**, *32*, 702.
[26] A. R. Abate, D. Lee, T. Do, C. Holtze, D. A. Weitz, *Lab Chip* **2008**, *8*, 516.
[27] J. K. Kim, K. Taki, M. Ohshima, *Langmuir* **2007**, *23*, 12397.
[28] P. van de Witte, P. J. Dijkstra, J. W. A. van den Berg, J. Feijen, *J. Membr. Sci.* **1996**, *117*, 1.

Received: November 23, 2008
Published online on February 2, 2009

